Design and Synthesis of Multifunctional Symmerical Squaraine Dyes for Molecular Photovoltaics by Terminal Alkyl-Chain Modifications

Kota Mori , Yuki Kurokawa , SHYAM S. PANDEY *

Posted Date: 23 April 2024

doi: 10.20944/preprints202404.1520.v1

Keywords: Dye-sensitized solar cells; Squaraine dye; Electrolyte effect; Terminal modification; Multifunctional; Dye sensitizer

 doi:10.20944/preprints202404.1520.v1

Article

Design and Synthesis of Multifunctional Symmerical Squaraine dyes for Molecular Photovoltaics by terminal Alkyl-Chain Modifications

Kota Mori *, Yuki Kurokawa and Shyam S. Pandey *

Graduate School of Life Science and Systems Engineering, Kyushu Institute of Technology, 2-4, Hibikino, Kitakyushu 808-0196, Japan; kurokawa.yuki207@mail.kyutech.jp (Y.K.)

* Correspondence: morik2371@gmail.com (K.M.); shyam@life.kyutech.ac.jp (S.S.P.)

Abstract: Novel far-red-sensitive symmetric squaraine (SQ) dyes with terminal alkyl-chain modifications were designed, synthesized and characterized aiming towards imparting multifunctionalities such as photosensitization, dye aggregation prevention and source of electrolyte components. The dye sensitizers **SQ-77** and **SQ-80** with the alkyl chain terminal modifications consisting of iodine and 1-methylimidazolium iodide, respectively, were designed and synthesized as new dye sensitizers for DSSCs based on the symmetric **SQ-5** without any terminal modification used as reference. Upon adsorption on the mesoporous TiO_2 surface, The SQ-77 depicted an enhanced dye loading and dye aggregation. On the other hand, **SQ-80** demonstrated reduced dye aggregation and stronger binding on the TiO_2 surface leading to enhanced durability of DSSCs. Apart from the most common photosensitization behaviour, the newly designed dye demonstrated multifunctionality such as aggregation prevention and electrolyte functionality utilizing iodine-based redox electrolyte in the presence and absence of I_2 and LiI additives. In the absence of LiI and I2, a mixture of **SQ-77** and **SQ-80** demonstrated a photoconversion efficiency of 1.54 % under simulated solar irradiation, which was about 6 times higher as compared to reference dye **SQ-5** (0.24 %) having no alkyl chai terminal modification.

Keywords: dye-sensitized solar cells; squaraine dye; electrolyte effect; terminal modification; multifunctional; dye sensitizer

1. Introduction

Adoption of renewable energy resources is getteing enhanced global attention to solve the future energy issues due to increasing energy demands owing to increasing population growth and standard of life aiming towards the development of a sustainable society. This attempt is demonstrated by the fact that the share of electricity generated from renewable energy sources in power generation has increased from 21.3% in 2012 to 29.9% in 2022. The installation of photovoltaic cells, a type of solar energy harvesting system, is being actively promoted, which has increased the amount of electricity generated in 2022 by 25% compared to the previous year, and they are almost equal to hydroelectric power generation. [1] However, there are some problems regarding installation locations due to the size and weight of the modules and how to treat them when they reach the end of their useful life. [2] On the other hand, research and development of next-generation solar cells, such as organic thin film/polymer solar cells, perovskite solar cells and dye-sensitized solar cells (DSSCs) have also geared momentum worldwide aimimng towards the realization of low-cost solar energy harvesting. [3–5] DSSCs have attracted much attention since their invention by O'Regan and Gräzel. [6] DSSCs have high potential due to their environmental friendliness, flexibility, simple manufacturing process, and efficient power generation capabilities under low intensity indoor light. [7–11] Common DSSCs are composed of a working electrode of nanocrystalline TiO_2 adsorbed with a sensitizing dye sensitizer, a counter electrode having electrocatalytic, and an

 doi:10.20944/preprints202404.1520.v1

electrolyte that fills the gap of both working and counter electrodes. Its photovoltaic conversion efficiency (PCE) is calculated by the multiplication of the short-circuit current density (Jsc), the open-circuit voltage (Voc), and the fill factor (FF). Since Jsc in DSSCs is determined by the optical absorption of sensitizing dyes, various efforts have been attempted by many researchers. The dyes used in DSSCs include inorganic and organic dyes, both of which currently exhibit conversion efficiencies of over 11%. [12–16]

The most well-known sensitizing dyes are those based on ruthenium complexes, with attractive features such as high stability. However, metal-based inorganic sensitizers have problems such as the use of precious metals, low molar absorption coefficients, and organic sensitizers are being actively investigated to compensate for these problems. Inorganic and organic dyes, which show high conversion efficiencies exceeding 10 %, have a relatively higher molar absorption coefficient absorbing light in the 300 nm to 700 nm wavelength region. The solution to this problem is to combine multiple dyes and extend the absorption region by co-sensitization. [17–19] Therefore, the development of dyes in the long wavelength especially in the near-infrared (NIR) wavelength region is inevitable for further enhancement in the PCE. Various classes of dyes such as polymethine, cyanine, phthalocyanine, porphyrins, and squaraine have been attempted recently to circumvent this issue. [20–23] The NIR dyes achieve long wavelength absorption by increasing π-conjugation, but their planar structure promotes dye aggregation and hampers the device performance of DSSCs. [24,25] Therefore, it is necessary to co-adsorb other materials with dye molecules on TiO2 to prevent dye aggregation but this leads to hampered dye loading, especially in the case of non-absorbing aggregation-preventing agents like most commonly used chenodeoxycholic acid. One of the well-adopted measures is to prevent aggregation by adding long alkyl chains to the dye. [26,27] Therefore, designing and developing novel sensitizing dyes with additional functionalities like aggregation prevention, surface passivation and assisting electrolyte functioning is necessary. Cobalt or copper complex-based electrolytes are used to achieve higher Voc. Their redox potentials are deeper than a typical iodine-based redox couple, and higher values can be expected in Voc, which is determined by the gap between the conduction band of TiO_2 and the redox potential of the electrolyte. However, unlike iodine-based redox couples, it is well known that cobalt- and copper-complexed redox couples, which are composed of cations, frequently suffer from the back electron transfer/ charge carrier recombination needing strict surface passivation and utilization of relatively thinner TiO_2 layer.

Therefore, The realization of high PCE by using these redox couples has been reported only with limited dyes. These dye molecules require alkyl chains as anti-dye-aggregation and special structures to prevent this reverse electron transfer. Despite these previous researches, very few studies have investigated the substitution of alkyl chain ends. So far, our research group has been actively involved in the design of the development of NIR dyes belonging to the squaraine family of dye-sensitizers. [28–31] Squaraine dyes are advantageous owing to versatile synthesis, easy tuning of energetics and optical absorption window and intense colour leading to their utilization for a wide range of applications, including photodynamic therapy, organic photovoltaics, ion sensors, fluorescent labels and probes. [32–36] In DSSCs, improving conversion efficiency and durability, ensuring safety, and reducing costs are unavoidable issues for their practical application. We have recently proposed multifunctional NIR dyes that demonstrated their suitability as sensitizers of DSSCs. [37] This was accomplished by substituting the long alkyl chain terminals of the dye main framework with iodine or imidazole, to impart multifunctionality such as prevention of dye aggregation and function as I2 in iodine-based electrolytes. In the present study, we designed, synthesized, and characterized a novel multifunctional dye (**SQ-80**) with 1-methylimidazolim iodide substituted at the alkyl chain terminal and these dyes were used as a sensitizer for DSSCs to investigate their photophysical characteristics.

 doi:10.20944/preprints202404.1520.v1

Materials and Methods

2.1. Materials

Lithium iodide (LiI) and iodine (I_2) were procured from Wako, Japan. Platinum catalyst precursor (Platisol T) and TiO_2 paste (Ti-nanoxide D/SP and T/SP) were procured from Solaronix. 4-tert-butylpyridine (t-BP) was procured from Sigma Aldrich. 1,2-dimethyl-3-propylene-imidazoliumdide, Squaric acid, 1-methylimidazole and other materials needed for the synthesis were procured from TCI Chemicals Japan. TB3017B resin, which is UV light-hardenable was procured from ThreeBond Japan.

2.2. Intermediates and Dyes Synthesis

The synthesis started utilizing an aromatic ring carboxy functionalized indole derivative 2,3,3-trimethyl-3H-indole-5-carboxylic acid following the procedure described by Pham et al. [38] The synthesis and characterization of symmetrical squaraine dyes, **SQ-5** and **SQ-77** have been reported previously. [37,39] The newly proposed dye **SQ-80** and the corresponding intermediate were synthesized according to **Scheme 1**.

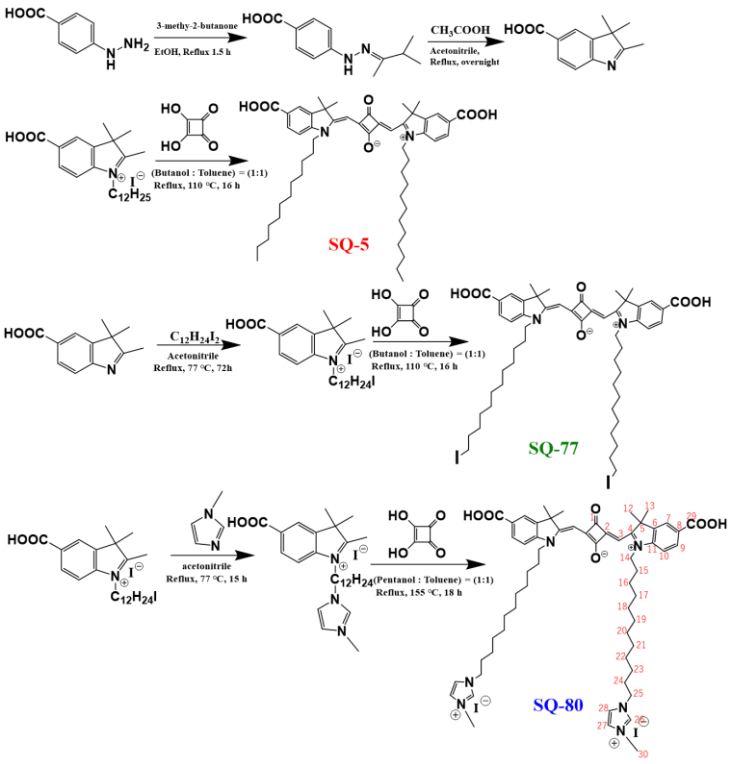

Scheme 1. Synthesis scheme of symmetrical SQ dye sensitizers.

2.2.1. Synthesis of 5-Carboxy-2,3,3-trimethyl-1-(12-1-methylimidazoledodecyl)-3H-indolium Iodide

1.2 g (2.3 mmol) of 5-Carboxy-2,3,3-trimethyl-1-(12-iodododecyl)-3H-indolium iodide and 360 mg (4.6 mmol) of 1-methylimidazole were dissolved in 30 mL of acetonitrile taken in 100 mL of a round-bottomed flask fitted with a condenser. For 12 hours, the reaction mixture was refluxed. After cooling the reaction mixture and evaporating the solvent, 1.42 g of red crude was obtained and purified by re-crystallization. HR-FAB-MS （C28H43N3O2 measured m/z : 454.6522 [M]+ ; calculated m/z : 454.8420 ; ） confirms the structural identity of this compound.

2.2.2. Synthesis of Symmetrical Squaraine Dye SQ-80

800 mg (1.8 mmol) of 5-Carboxy-2,3,3-trimethyl-1-(12-1-methylimidazoledecyl)-3H-indolium iodide and 100 mg (0.88 mmol) of squaric acid were dissolved in 30 mL of toluene-pentanol (1:1)

 doi:10.20944/preprints202404.1520.v1

mixture taken in 100 mL of a round-bottomed flask fitted with a condenser. For 12 hours, the reaction mixture was refluxed. After cooling the reaction mixture and evaporating the solvent, the product was purified using silica gel column chromatography with an eluting solvent of acetone, water, and acetic acid, yielding 167 mg of dark blue solid in a 19% yield. FAB-MS (for C60H81N6O6, measured m/z: 981.63 [M]+; calculated m/z: 981.35;) and 1H NMR (500 MHz, CD3OD): δ/ppm = 7.93 (d, 2H, Ar-H); 7.91(s, 2H, Ar-H); 7.53(d, 2H, Ar-H); 7.46(s, 2H, Ar-H); 7.13(d, 2H, Ar-H); 7.11(d, 2H, Ar-H); 5.91(s, 2H, CH); 4.07(t, 4H, CH2); 4.06(t, 4H, CH2); 4.04(t, 4H, CH2); 3.83(s, 2H, CH); 1.72(d, 4H, CH2); 1.65(s, 12H, CH3); 1.32(m, 4H, CH2); 1.26(m, 4H, CH2); 1.14(m, 24H, CH2); 13C NMR (CD3OD) 184.40 (C1), 177.31 (C4), 173.66 (C29), 145.68 (C2), 142.69 (C11), 138.03 (C6), 137.77 (C26), 134.30 (C8), 131.19 (C7), 124.91 (C9), 124.42 (C27), 123.63 (C28), 110.61 (C10), 88.03 (C3), 50.81 (C5), 50.31 (C14), 44.78 (C25), 36.46 (C30), 31.16 (C24), 30.46 (C18-21), 30.30 (C17, 22), 28.06 (C15), 27.58 (C16), 27.38 (C23) 27.27 (C12,13); confirms the structural identity of dye.

2.2.5. Characterizations of Synthesized SQ-80

The synthesized intermediate and final dye were characterized by Fast Ion Bombardment (FAB)-mass spectrometry in the positive ion monitoring mode to confirm structural identity. Synthesized dyes were dissolved in deuterated methanol to record nuclear magnetic resonance (NMR) spectra using an NMR spectrometer (JEOL, 500 MHz) to confirm the final structure. The electronic absorption spectra were measured in solution and on TiO_2 film using a UV-vis-NIR spectrophotometer (JASCO V-550). Using cyclic voltammetry (CV), the dye's highest occupied molecular orbital (HOMO) energy level was ascertained. The CV measurements were performed using an auto polarization system (HSV-100, Hakuto Denko, Japan). The ferrocene (Fc) and 1 mM of each synthesized dye in DMF were used for the CV measurement. 100 mM tetrabutylammonium hexafluorophosphate was also added as the electrolyte. The difference in the oxidation potential of the reference Fc+/Fc redox pair and the synthesized dye estimated the HOMO energy levels of the synthesized dye. The energies associated with the synthesized dye's optical band edge (Eg) were estimated using absorption spectra of dye-adsorbed TiO_2 thin films. The lowest unoccupied molecular orbital (LUMO) energies were calculated from these values. 40 mM NaOH solution: acetonitrile: t-butanol: ethanol (1:1:1, v/v) was used to remove the dye adsorbed on TiO_2 and the presence of the dye was measured by spectrophotometer comparing to the dye when dissolved in the same solution to estimate the number of dye molecules adsorbed on the TiO_2 layer.

2.3. Fabrication and Characterization of DSSCs

2.3.1. Device Fabrication

Subsequent to a 30-minute UV/O_3 treatment, detergent water, distilled water, acetone and 2-propanol were used to ultrasonically clean Fluorine-doped Tin Oxide (FTO) glass substrates (10 Ohm/sq). Before sintering in the muffle furnace (FO100, Yamato Co., Ltd.) for 45 minutes at 450 °C, cleaned substrates were soaked in 40 mM $TiCl_4$ aqueous for an hour at 70 °C ($TiCl_4$ treatment). They were then rinsed with distilled water and ethanol. To obtain a 12 μm TiO_2 layer, Ti-nanoxide T/SP was printed on substrates treated with $TiCl_4$ using a screen printer and sintered for 45 minutes at 500 °C using a muffle furnace then, Ti-nanoxide D/SP was printed and sintered on mesoporous TiO_2 at same condition for T/SP. The TiO_2-coated substrates were done $TiCl_4$ treatment again. Then, the substrates were soaked for four hours in a solution containing synthesized dyes (0.2 mM) and CDCA (10 mM) in ethanol. After dye absorption, they were rinsed with ethanol to remove any dye molecules that had not been adsorbed on TiO_2. The same procedure as previously mentioned was used to clean pre-drilled FTO glass substrates. The solution containing precursor of Pt catalyst (Platisol T) was applied by spin-coating for 10 seconds at 1400 rpm and sintered for 30 minutes at 500 °C. The working and counter electrodes were sandwiched using a hot melt spacer (25 μm). Subsequently, the pre-drilled hole on the counter electrode was used to inject the iodine-based redox electrolyte (I_3^-/I^-), which was composed of lithium iodide (100 mM), iodine (50 mM), 1,2-dimethyl-3-propylene-

 doi:10.20944/preprints202404.1520.v1

imidazoliumdide (600 mM) and t-BP (500 mM) in acetonitrile. Finally, the DSSCs were sealed using TB3017B resin.

2.3.2. Device Characterization

The photocurrent density–voltage (J–V) curves were measured under 100 mW/cm^2 of simulated solar irradiation using a solar simulator (CEP-2000 Bunko Keiki Co. Ltd, Japan) with a xenon lamp (Bunko Keiki BSO-X150LC). Additionally, 100 mW/cm^2 simulated solar irradiation was measured using a common calibration Si photodetector (BS-520 S/N 007, Bunko-Keiki, Japan). The active area of DSSCs was controlled at 0.25 cm^2 using a black metal mask. The photocurrent at each wavelength range was measured by monochromatic light irradiation using an action spectrum measurement system connected to a solar simulator (CEP-2000, Bunko Keiki, Japan). The amount of light in each wavelength range was calculated from the sensitivity of a calibration silicon solar cell (S1337, Bunko Keiki, Japan) and measured photocurrent of S1337 in each wavelength range. Then, the photocurrent of the sample was measured at each wavelength range and the incident photon-current conversion efficiency (IPCE) was calculated. The Electrochemical impedance spectroscopic (EIS) experiment was performed using a frequency response analyzer (Solartron Analytical, 1255B) coupled to a potentiostat (Solartron Analytical, 1287) between 0.1 and 10^5 Hz under the same irradiation in J-V curves measurement. EIS data was analyzed using Bode and Nyquist plots to examine each interfacial resistance.

3. Results and Discussion

3.1. Electronic Absorption Spectra

Figure 2(a) shows the electronic absorption spectra of synthesized symmetric squaraine dyes (10 μM in ethanol). It shows that dyes have highly narrow, strong, and sharp light absorption, primarily in the 550 nm to 700 nm wavelength region. Because the primary π-conjugated framework of all three dyes is the same, the absorption maximum (λ_{max}) was almost the same appearing at 646 nm. These squaraine dyes also exhibit a shoulder in the solution state, a common feature of squaraine dyes, at a 550–650 nm wavelength. It was found that the molar extinction coefficient varied depending on the type of terminal substituents, even though the λ_{max} was identical. Compared to the standard SQ-5, SQ-77, bearing the terminal with iodine, showed a dark colour. On the other hand, **SQ-80** with a modified terminal consisting of 1-methylimidazole showed a pale color compared to SQ-5. An analysis of dye adsorption behaviour on mesoporous TiO_2 surfaces provides important findings regarding dye aggregation that must be controlled to improve photon harvesting and maximize DSSC performance. **Figure 2(b)** shows the normalized electronic absorption spectra of the synthesized dyes adsorbed on a transparent 4 μm TiO_2 and Table 1 shows summarized optical parameters from **Figure 2**.

 doi:10.20944/preprints202404.1520.v1

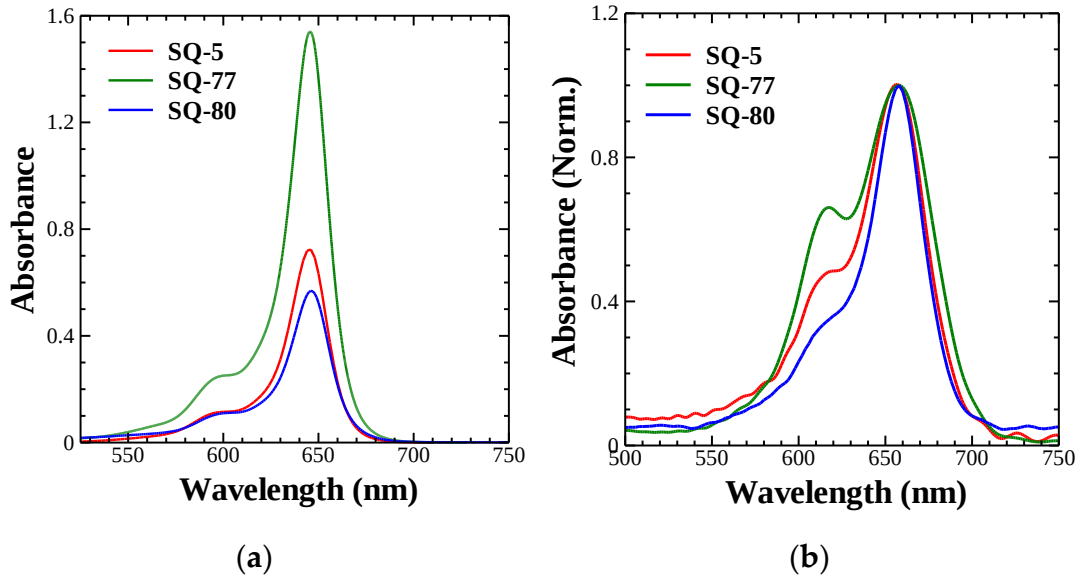

Figure 2. (a) the electronic absorption spectra of the synthesized symmetrical squaraine dyes (10 μM in ethanol) and (b) the normalized absorption spectra of dye absorbed transparent TiO_2 (4 ⍵m).

Table 1. The extracted optical parameters of synthesized symmetrical SQ dyes are from Figure 2.

Dye	λ_{max} (solution)	ε (solution) ($dm^3.mol^{-1}.cm^{-1}$)	λ_{max} (TiO_2)	Absorption Edge nm (eV)	Aggregation index	Dye loading ($nmol/cm^2$)	Dye desorption rate ($nmol/cm^2/min$)
SQ-5	646 nm	1.45 x 10^5	658 nm	710 nm (1.75 eV)	0.48	29.3	5.86
SQ-77	646 nm	3.08 x 10^5	658 nm	715 nm (1.73 eV)	0.66	54.0	6.00
SQ-80	646 nm	1.18 x 10^5	658 nm	720 nm (1.72 eV)	0.32	35.6	2.09

The solid-state electronic absorption spectrum was broadened and redshifted compared to the absorption spectrum of squaraine dye in ethanol solution shown in **Figure 2(a)**. This indicates dye aggregation and interaction between TiO_2 surface and dye molecules. [40] The λmax values were the same for the alkyl terminal substitutions (H, I, 1-methylimidazole). However, the spectral broadening and optical absorption edge changed, indicating differences in the dye molecule aggregation on the TiO2 surface. The Vibronic shoulder seen in **Figure 2(b**) at 610 nm in solution is more noticeable in solid state than in solution and is thought to be caused by the dye aggregate formation. [41] The ratio of the absorbance at 610 nm (aggregation) and 658 nm (monomeric dye) was utilized to estimate the relative extent of the dye aggregation.[42] It is clearly shown from the normalized solid-state absorption spectrum that the 1-methylimidazole at the terminal of the alkyl chain in **SQ-80** exhibits an aggregation index of 0.32, which is smaller than **SQ-5** without terminal modification (0.48) and **SQ-77** with terminal iodine modification (0.66). This suggests that the 1-methylimidazole group increased the intermolecular distance and decreased the electrostatic interaction among the dye molecules hampering the dye aggregation. Since the alkyl chain length is the same, hampered dye aggregation for **SQ-8**0 indicates the role of imidazolium iodide terminal functionality in dye aggregation prevention.

 doi:10.20944/preprints202404.1520.v1

3.2. Adsorption of Dye Molecules on TiO_2

Experiments of dye adsorption and desorption were conducted to measure the amount of dye adsorbed on TiO_2 and the strength of binding of dye molecules TiO_2 surface alongwith summarization of results in Table 1. To determine the total loading of dye adsorbed on TiO_2, dye molecules were fully adsorbed on the TiO_2 surface and then completely desorbed using a mixed solution consisting of acetonitrile, tert-butanol, water, and NaOH (1:1:1:1 v/v). Synthesized SQ dye sensitizers were adsorbed on the TiO_2 to estimate dye stability. The quantity of dye desorbed within a designated time was calculated using spectrophotometry. **Table 1** shows that, even under the same dye desorption circumstances (TiO_2 thickness and area and dipping time duration). The binding strength of each synthesized dye sensitizer onto mesoporous TiO_2 was not the same. Due to their comparatively quick dye desorption (5.86 and 6.00 nmol/cm^2/min) for **SQ-5** and **SQ-77**, respectively, **SQ-80** exhibited nearly three times stronger binding on TiO2 surface (2.09 nmol/cm^2/min).

3.3. Cyclic Voltammetry

In DSSC studies, cyclic voltammetry (CV) is used not only for electrochemical characterization of dye-sensitizers but also to estimate the energetics of sensitizing dyes to judge their suitability as a sensitizer. **Figure 3** shows CV recordings of each synthesized SQ dye and ferrocene (Fc) as the standard reference in dimethylformamide (DMF) solution using similar electrochemical cell conditions such as electrodes, electrolytes, and scan rates. The energy of the highest occupied molecular orbital (HOMO) of the dyes was calculated using the shift of the first oxidation peak of the dye relative to the Fc/Fc^+ redox pair used as a reference. It is widely recognized that the redox potential of the Fc/Fc^+ redox pair is 0.403 V with respect to a saturated calomel electrode, which is equivalent to -5.09 eV from the vacuum level. [43] The oxidation potentials of ferrocene, **SQ-5**, **SQ-77**, and **SQ-80** were found to be 0.45 V, 0.42 V, 0.50 V, and 0.48 V, respectively. The results showed that the synthesized dyes shifted -0.03, +0.05, and +0.03, respectively, compared to the first oxidation potential of ferrocene. From the redox potential of -5.09 eV for Fc/Fc^+, the estimated values of the HOMO energy were -5.06 eV, -5.14 eV and -5.12 eV for the **SQ-5, SQ-77** and **SQ-80**, respectively.

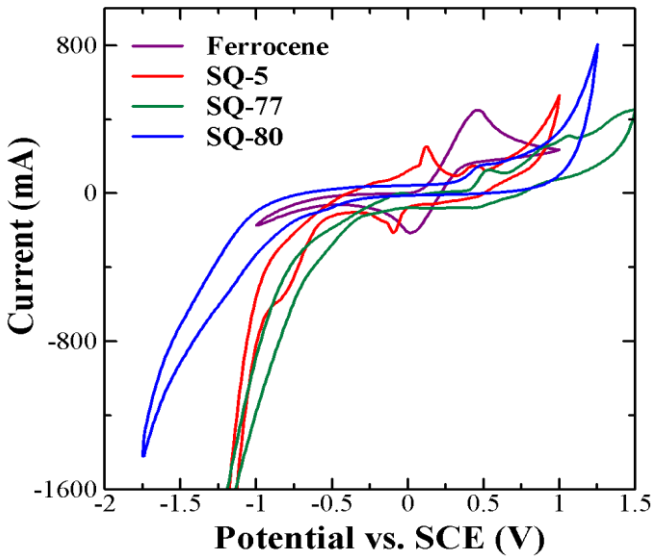

Figure 3. Cyclic voltammograms of ferrocene and symmetrical SQ dyes in I_3^-/I^- redox electrolyte (Scan rate was 50 mVs^{-1}).

3.4. Energy Band Diagram

In addition to strong light absorption, presence of suitable anchoring group, and favorable electrochemical bonding with TiO_2, the dye sensitizer of DSSCs must demonstrate energetic matching for the electron transporting wide bandgap semiconductor and redox electrolyte (TiO_2 and I^-/I_3^- in the

 doi:10.20944/preprints202404.1520.v1

present case) for the facile electron injection and dye regeneration, respectively. Table 1 also summarizes the estimated values of the energy band gap (Eg) estimated from the onset of the optical absorption edge of **Figure 2(b)**. The energy of the lowest unoccupied molecular orbital (LUMO) was estimated using the relation LUMO = HOMO + Eg. Based on earlier publications, the conduction band (CB) energy of TiO_2 and the redox energy level of the I^-/I_3^- electrolyte was reported to be – 4.00 eV and – 4.90 eV, respectively, which was used in the energy band diagram depicted in **Figure 4**. [44] The LUMO energies of all synthesized SQ dyes were higher than the TiO2 CB, with a driving force of 0.6-0.7 eV that allows easy electron injection from the LUMO of photoexcited dye molecules into the TiO2. Compared to the standard **SQ-5,** the LUMO of **SQ-77** and **SQ-80** (terminal substitution) were decreased. Decreases in LUMO have been reported with terminal substitution of alkyl chains.[37,45] In addition, the HOMO energy levels of synthesized dye were lower than the iodide/triiodide redox potential, suggesting that dye regeneration may easily occur following the injection of electrons of photoexcited dye molecules into TiO_2.

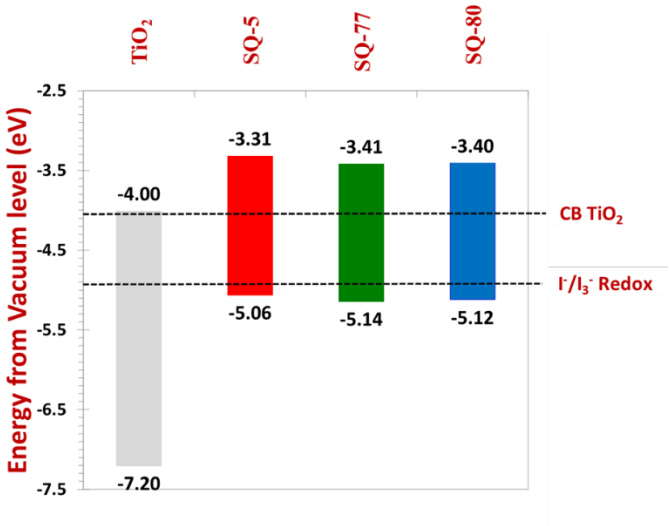

Figure 4. Energy band diagram of the symmetrical SQ dyes to justify their suitability as sesnitizer with TiO_2 as electron acceptor and I^-/I_3^- redox electrolyte.

3.5. Photovoltaic Characterization

The current density-voltage (J-V) characteristics of DSSCs for evaluating their photovoltaic performances using different SQ dyes are shown in **Figure 5(a)**. These measurements were carried out under solar irradiation of 100 mW/cm^2. Based on the J-V characteristics, photovoltaic metrics such as PCE, fill factor (FF), open-circuit voltage (V_{oc}), and short-circuit current density (J_{sc}) were calculated and presented in **Table 2.** The DSSCs with the **SQ-5** dye recorded the highest PCE of 4.2 % among the three dyes with Jsc, Voc, and FF of 11.98 mA/cm^2, 0.61 V, and 0.57, respectively. Additionally, the alkyl chain terminal modified with iodine dye (**SQ-77**) and terminal 1-methylimidazole-modified (**SQ-80**) showed a slightly lower PCE of 3.8 and 3.7 %, respectively. Despite the higher dye loading in the case of **SQ-77** , its PCE as well as Jsc was lower than that of DSSCs based on **SQ-5**. This could be attributed to enhanced aggregation of **SQ-77** with aggregation index of 0.66 as compared to that of **SQ-5** with an aggregation index of 0.48 as shown in Table 1. On the other hand, despite decreased dye loading in the case of **SQ-80** (35.6 nmol/cm^2) as compared to that of **SQ-77** (54 nmol/cm^2), their photovoltaic performances are nearly similar. This could be explained by considering the compensation of reduced dye loading by decreased dye aggregation in the case of **SQ-80** as compared to that of **SQ-77**. It has been reported that monomeric dyes exhibit enhanced electron injection as compared to that of dye aggregates hampering the Jsc as well as PCE of the DSSCs. [46] The IPCE spectrum provides information on the photon harvesting behavior of dye molecules for each wavelength, so monochromatic light is used for this measurement. **Figure 5(b)** shows the incident

 doi:10.20944/preprints202404.1520.v1

photon to current conversion efficiency (IPCE) spectra of DSSCs using **SQ-5**, **SQ-77**, and **SQ-80**. Since the peak about 350 nm is due to TiO_2 absorption, the values of the peaks were nearly identical, representing 50% of each dye. The results showed that the maxima were 68 % at 658 nm for all of the three dyes. The photon harvesting was demonstrated in the actual fabricated DSSCs although the synthesized SQ dyes did not demonstrate light absorption in the 400-500 nm range in **Figure 2. SQ-77** demonstrated the largest photon harvesting in this range, while **SQ-80** demonstrated the smallest. It is also the same trend of dye aggregation as discussed in section 3.1.

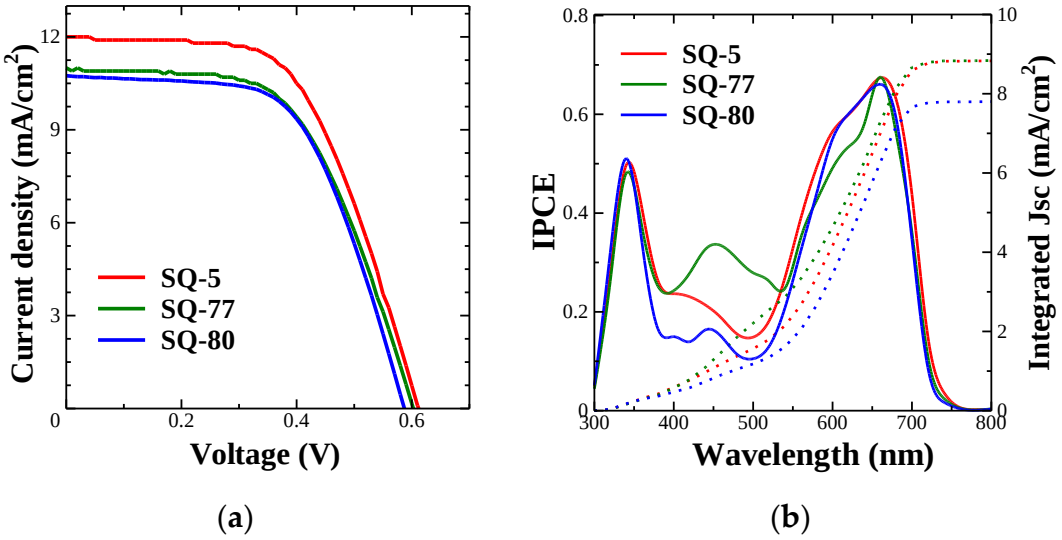

Figure 5. (a) J-V curves and (b) IPCE spectra of DSSCs using SQ dye sensitizer with different terminal substitutions.

Table 2. Photovoltaic parameters for DSSCs using different dye-sensitizers.

Dye	J_{sc} (mA/cm²)	V_{oc} (V)	FF	PCE (%)
SQ-5	12.0	0.62	0.57	4.21
SQ-77	11.0	0.61	0.56	3.77
SQ-80	10.7	0.59	0.59	3.74

3.6. Electrochemical Impedance Spectra

When examining the charge-transfer process occurring at various interfaces, DSSC research has extensively used the electrochemical impedance spectroscopic (EIS) technique. Rs in the Nyquist plot represents the almost identical sheet resistance of the FTO substrate. DSSCs are made up of three main impedance parts. The interface between the platinum used as the counter electrode and the electrolyte is represented by component 1 (R1); the interface between the TiO2 semiconductor used as the working electrode and dye and the electrolyte is represented by component 2 (R2); and the impedance resulting from the behaviour of the electrons in the electrolyte near the electrode is represented by component 3 (R3). [47,48] The DSSCs fabricated using different SQ dyes under investigation were subjected to EIS measurement and obtained corresponding Bode and Nyquist plots are shown in **Figure 6**. The electrical parameters that were fitted using an equivalent circuit or calculated from the EIS measurement are shown in **Table 3**. There were no significant differences in Rs and R2 between the three dyes. It matched the theory of general EIS analysis for DSSCs. The plot for SQ-77 was not the same due to higher resistance than the other two dyes. One possible reason is that a portion of the dye aggregation, which was not directly absorbed on TiO2 and was not removed by rinsing before DSSCs assembly, dissolved into the acetonitrile electrolyte and prevented charge transfer at the catalyst/electrolyte interface. The connection between each arc in the Nyquist plot of SQ-80 was smooth, and each interface was difficult to identify compared to the other dyes. In addition, the R3 estimated by fitting, which should indicate electrolyte diffusion, was very small.

 doi:10.20944/preprints202404.1520.v1

However, this also implies that SQ-80 may also play a role as an electrolyte more than other dyes. It is possible that the R3 peak shifted to a lower frequency over the range for the measurement. The relationship $\tau = 1/2\pi fp$, where fp is the peak at a lower frequency in Bode plots, can be used to compute the electron lifetime[30]. Since electron lifetime is proportional to peak frequency, it increases with decreasing peak frequency. SQ-80 (τe = 4.22 ms) has a shorter electron lifetime than **SQ-5** and **SQ-77** (τe = 8.41, 5.31 ms). It indicates that the **SQ-80** DSSC can lessen charge recombination because, as previously mentioned, increased dye aggregation hinders electron injection.

Table 3. The summarized electrical parameters of DSSCs fabricated using different dyes deduced from EIS analysis shown in Figure 6.

Dye	R_s (Ω)	R_1 (Ω)	R_2 (Ω)	R_3 (Ω)	fp (Hz)	τ_s (ms)
SQ-5	27.5	9.42	20.3	1.30	18.9	8.41
SQ-77	24.0	26.7	18.0	3.35	30.0	5.31
SQ-80	29.2	12.0	16.9	0.53	37.8	4.22

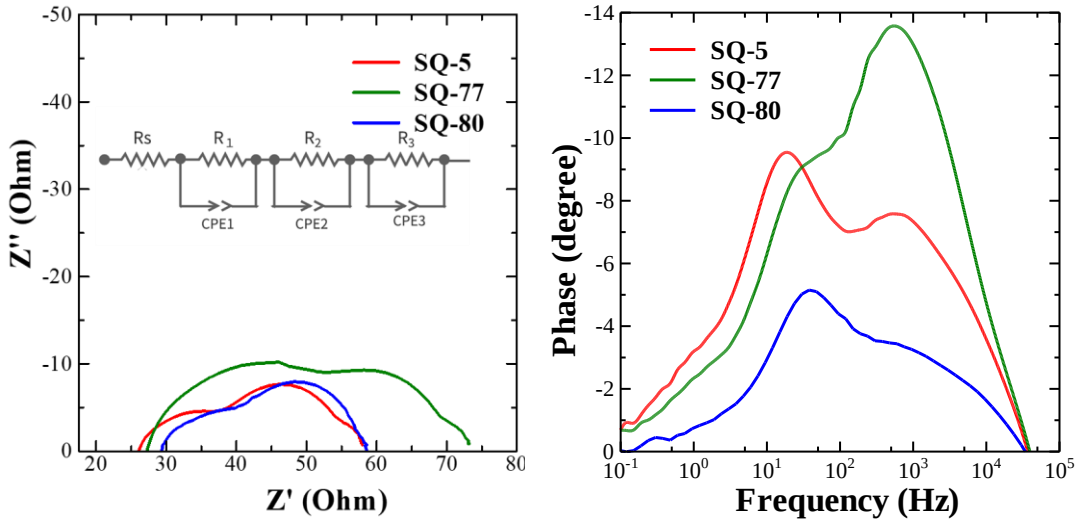

Figure 6. (a) Nyquist plots and equivalent circuits for data fitting and (b) Bode plots of the DSSCs using symmetrical SQ dye sensitizers.

3.7. Relative Durability of DSSCs

In DSSCs, durability evaluation is an important factor for practical application. The durability includes volatilization of the electrolyte, degradation of Pt, the catalyst used for the counter electrode, and dye desorption. After preparing DSSCs with four samples, each of SQ-5 and SQ-80, the DSSCs were stored in a desiccator in the dark and DSSC performance was measured after the storage of time of 0, 100, 200, 300, and 450 hours. **Figure 7** shows the J-V curves and tracked PCE with time along with the summarization of photovoltaic parameters in **Table 4**. DSSC with **SQ-5** resulted in a 48 % reduction in PCE at 450 hours compared to 0 hours. On the other hand, **SQ-80** maintains 78% PCE after 450 hours, indicating that SQ-80 is relatively more stable with higher durability. The decrease in PCE for these two dyes is mainly due to decreased J_{SC} for **SQ-5**, which was 60 % maintaining 40 % after 450 hours. On the other hand, DSSCs based on **SQ-80** retained 67 % of the Jsc after 450 hours. The decrease in Jsc can be attributed to the degradation of the dyes, and this significant difference between **SQ-5** and **SQ-80** can be attributed to the intensity of dye desorption described in Section 3.2

 doi:10.20944/preprints202404.1520.v1

and Table 1. One factor in dye desorption is the intrusion of water molecules. To solve this problem, there is an approach in which the dye molecule has long alkyl chains. **SQ-80** has long alkyl chains, and the bulky 1-methylimidazole at the alkyl chains terminal is thought to further prevent water from entering the dye.

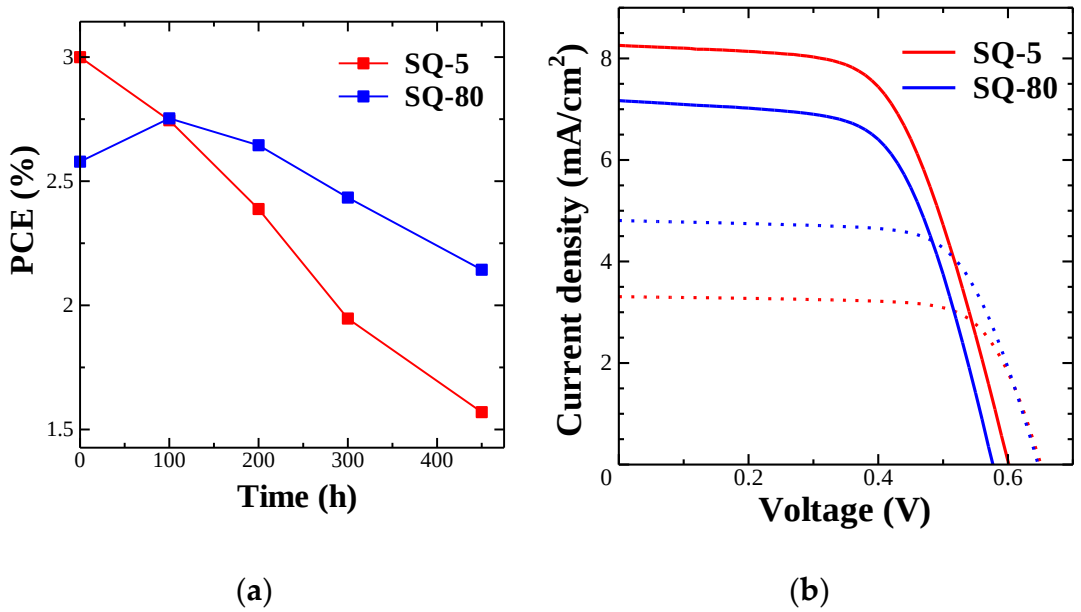

Figure 7. (a) The tracked PCE as function of time and (b) photovoltaic characteristics (solid line: 0 hours, dotted line: 450 hours) of the DSSCs using symmetrical SQ dye sensitizers (SQ-5 and SQ-80).

Table 4. The summarized photovoltaic parameters deduced from J-V characteristics of Figure 7 (b). (These parameters were calculated standard deviations using four samples prepared with the same conditions.).

Dye	Time (h)	J_{sc} (mA/cm²)	V_{oc} (V)	FF	PCE (%)
SQ-5	0	8.26 (± 0.90)	0.61 (± 0.01)	0.60 (± 0.02)	3.00 (± 0.23)
	450	3.31 (± 0.18)	0.66 (± 0.01)	0.72 (± 0.002)	1.57 (± 0.11)
SQ-80	0	7.17 (± 0.32)	0.583 (± 0.005)	0.618 (± 0.02)	2.58 (± 0.12)
	450	4.81 (± 0.46)	0.65 (± 0.01)	0.67 (± 0.031)	2.14 (± 0.14)

3.8. Verification of Electrolyte Functionality by Mixture of SQ-77 and SQ-80 Dyes

We have already reported the electrolyte effect of the dye molecule itself, which demonstrated that DSSCs worked without Iodine in electrolytes using the terminal iodine modification of **SQ-77**. Interested by this observation, **SQ-80** dye was designed and synthesized bearing 1-methylimidazole at the alkyl chain terminal expecting this dye to play an important role as the electrolyte component in the iodine-based electrolyte. To demonstrate the electrolyte effect, the blended **SQ-77** and **SQ-80** dyes owing to their terminal modification as a source of iodine and I- for iodine-based redox electrolyte. The reference dye **SQ-5** without any terminal modification of the alkyl chain was used at different concentrations of I2 and LiI in the electrolyte. Dimethyl-3-propyleneimidazolium iodide (600 mM), I2 (50 mM, 0 mM), and LiI (100 mM, 0 M) in acetonitrile were used to prepare the redox

 doi:10.20944/preprints202404.1520.v1

electrolyte for the present investigation. **Figure 8** and **Table 5** show the J-V curves and corresponding photovoltaic parameters for DSSC with mixed dyes (**SQ-77**:**SQ-80** = 1:1, 1:4, 4:1) and reference dye **SQ-5** at different concentrations of I2 and LiI in the electrolyte, respectively. There is no significant difference in the PCE of the four DSSCs with normal iodine electrolytes (I2 50 mM, LiI 0.1 M). However, in I2 and LiI-free electrolytes, there is a marked difference between the mixed dye (**SQ-77**, **SQ-80**) and reference dye **SQ-5**. DSSC with mixed dye (SQ-77:SQ-80 = 1:4) showed Jsc, Voc, and FF of 4.60 mA/cm2, 0.730 V, and 0.453, respectively, and 1.53 % under simulated solar irradiation, while DSSC with **SQ-5** showed highly hampered PCE of only 0.24 % under simulated solar irradiation. This significant decrease in FF could be due to a lack of iodine in the electrolyte. [49,50] From these results, we can say that I2 and LiI play a role in the electrolyte in the mixed dyes (**SQ-77**, **SQ-80**). In addition, the conversion efficiency increases as the ratio of **SQ-80** increases in three different dye mixtures (**SQ-77**:**SQ-80** = 1:1, 1:4, 4:1). This is because **SQ-80** plays a role of the I- source and as shown in equation (1), an increase in the concentration of I- promotes the formation of I3-, facilitating the formation of an I-/I3- redox couple. When 500 mM LiI and 50 mM I2 are added in acetonitrile, as shown in equation (2), K is high, I2 reacts with I- to form I3-, and the free iodine concentration is very low. [51,52]

$$I_2 + I^- = I_3^- \quad (1)$$

$$K = \frac{[I_3^-]}{[I_2]\,[I^-]} = 10^{6.76} \quad (2)$$

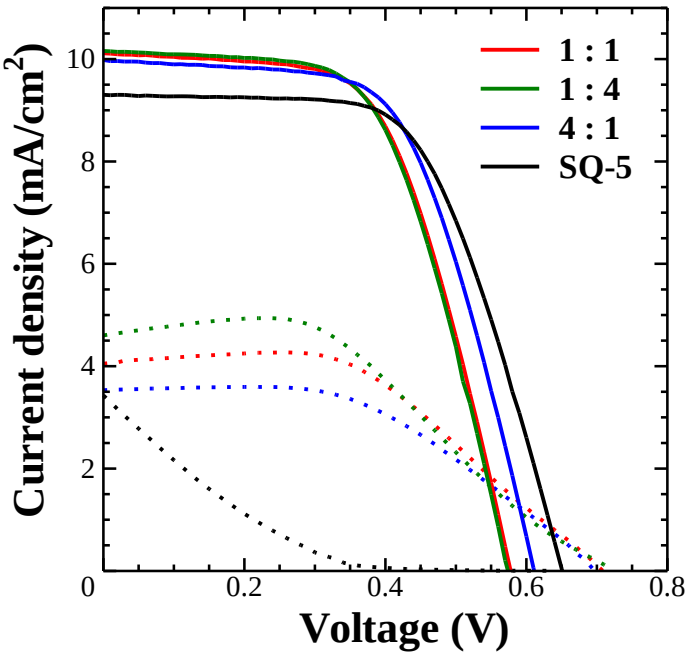

Figure 8. J-V curves of blended dye sensitizer (SQ-77 and SQ-80) and SQ-5 DSSCs with different concentrations of I2 and LiI electrolyte injection. (solid line: normal iodine electrolyte, dotted line: I_2 and LiI free electrolyte).

Table 5. The summarized photovoltaic parameters for DSSCs estimated from the J-V characteristics shown in Figure 8.

SQ-77: SQ-80	I_2 and LiI conc. (mM)	J_{sc} (mA/cm²)	V_{oc} (V)	FF	PCE (%)
1 : 1	50, 100	10.1	0.58	0.59	3.48
1 : 4		10.0	0.62	0.60	3.68

 doi:10.20944/preprints202404.1520.v1

4 : 1		10.2	0.58	0.59	3.46
SQ-5		9.30	0.66	0.60	3.70
1 : 1	0, 0	4.05	0.71	0.51	1.45
1 : 4		4.60	0.73	0.45	1.52
4 : 1		3.87	0.70	0.52	1.41
SQ-5		3.43	0.64	0.11	0.24

4. Conclusions

In this study, the terminal modification of the alkyl chain in the squaraine dye was carried out aiming towards their multifunctional role as sensitizer and electrolyte component source was successfully demonstrated. This is expected to reduce the number of materials used in DSSCs, leading to lower costs and process savings. Three symmetrical SQ dye sensitizers with various modifications at their alkyl chain terminal, like iodine and 1-methylimidazole, have been made and used as dye sensitizers for the use of DSSCs. Multiple investigations have been conducted on their photophysical, electrochemical, and photovoltaic characteristics. **SQ-77** (modified alkyl chain terminal by iodine) demonstrated a hyperchromic effect and enhancement of the dye molecule aggregation compared to **SQ-5**. Meanwhile, **SQ-80** (modified alkyl chain terminal by 1-methylimidazole) demonstrated the prevention of dye molecule aggregation. The highest PCE in DSSCs prepared with these dyes was 4.2% with **SQ-5** (unmodified) although the PCE of **SQ-77** and **SQ-80** was only about 10% lower than **SQ-5**. On the other hand, DSSCs with **SQ-80** demonstrated higher PCE than **SQ-5** after 450 hours of storage and improved binding strength on the TiO_2 surface. These findings demonstrate that the interfacial charge transport and durability of squaraine dye are influenced by the architectures of the Alkyl chain terminal functionalization. The blend dyes SQ-77 and SQ-80 demonstrated about 1.5 % PCE, which is 5 times higher than SQ-5 when iodine and LiI were not included in the electrolyte. It is likely to be attributed to the I^-/I_3^- redox couple generated by the iodine and 1-methylimidazole modified at the alkyl chain terminals of the dyes and DSSCs operated normally.

References

1. REN21. *Renewables 2023 Global Status Report Collection, Global Overview*; 2023 (page 14 and 17).
2. Deng, R.; Chang, N. L.; Ouyang, Z.; Chong, C. M. A Techno-Economic Review of Silicon Photovoltaic Module Recycling. *Renewable and Sustainable Energy Reviews*. **2019,** 109, 532-550; DOI:10.1016/j.rser.2019.04.020.
3. Kokkonen, M.; Talebi, P.; Zhou, J.; Asgari, S.; Soomro, S. A.; Elsehrawy, F.; Halme, J.; Ahmad, S.; Hagfeldt, A.; Hashmi, S. G. Advanced Research Trends in Dye-Sensitized Solar Cells. *Journal of Materials Chemistry A*. **2021**, 9, 10527-10545; DOI:10.1039/d1ta00690h.
4. Zhao, C.; Wang, J.; Jiao, J.; Huang, L.; Tang, J. Recent Advances of Polymer Acceptors for High-Performance Organic Solar Cells. *Journal of Materials Chemistry C*. **2019**, 8, 28-43; DOI:10.1039/c9tc05567c.
5. Chen, Y.; Zhang, L.; Zhang, Y.; Gao, H.; Yan, H. Large-Area Perovskite Solar Cells-a Review of Recent Progress and Issues. *RSC Advances*. **2018**, 8, 10489-10508; DOI:10.1039/c8ra00384j.
6. O'Regan, B.; Grätzel, M. A Low-Cost, High-Efficiency Solar Cell Based on Dye-Sensitized Colloidal TiO_2 Films. *Nature* **1991**, 353, 737–740; DOI:10.1038/353737a0.
7. Maddah, H. A.; Berry, V.; Behura, S. K. Biomolecular Photosensitizers for Dye-Sensitized Solar Cells: Recent Developments and Critical Insights. *Renewable and Sustainable Energy Reviews*. **2020**, 121, 109678; DOI:10.1016/j.rser.2019.109678.
8. Bella, F.; Gerbaldi, C.; Barolo, C.; Grätzel, M. Aqueous Dye-Sensitized Solar Cells. *Chemical Society Reviews*. **2015**, 44, 3431-3473; DOI:10.1039/c4cs00456f.

9. Wang, C.; Zhang, X.; Cao, D.; Yin, H.; Li, X.; Cheng, P.; Mi, B.; Gao, Z.; Deng, W. In Situ Preparation of Hierarchically Structured Dual-Layer TiO_2 Films by E-Spray Method for Efficient Dye-Sensitized Solar Cells. *Org. Electron.* 2017, 49, 135-141; DOI:10.1016/j.orgel.2017.06.002.
10. Parisi, M. L.; Dessì, A.; Zani, L.; Maranghi, S.; Mohammadpourasl, S.; Calamante, M.; Mordini, A.; Basosi, R.; Reginato, G.; Sinicropi, A. Combined LCA and Green Metrics Approach for the Sustainability Assessment of an Organic Dye Synthesis on Lab Scale. *Front. Chem.* **2020**, 8, 214; DOI:10.3389/fchem.2020.00214.
11. Michaels, H.; Rinderle, M.; Freitag, R.; Benesperi, I.; Edvinsson, T.; Socher, R.; Gagliardi, A.; Freitag, M. Dye-Sensitized Solar Cells under Ambient Light Powering Machine Learning: Towards Autonomous Smart Sensors for the Internet of Things. *Chem. Sci.* **2020**, 11, 2895-2906; DOI:10.1039/c9sc06145b.
12. Han, L.; Islam, A.; Chen, H.; Malapaka, C.; Chiranjeevi, B.; Zhang, S.; Yang, X.; Yanagida, M. High-Efficiency Dye-Sensitized Solar Cell with a Novel Co-Adsorbent. *Energy Environ. Sci.* **2012**, 5, 6057-6060; DOI:10.1039/c2ee03418b.
13. Kang, S. H.; Jeong, M. J.; Eom, Y. K.; Choi, I. T.; Kwon, S. M.; Yoo, Y.; Kim, J.; Kwon, J.; Park, J. H.; Kim, H. K. Porphyrin Sensitizers with Donor Structural Engineering for Superior Performance Dye-Sensitized Solar Cells and Tandem Solar Cells for Water Splitting Applications. *Adv. Energy Mater.* **2017**, 7, 1602117; DOI:10.1002/aenm.201602117.
14. Mathew, S.; Yella, A.; Gao, P.; Humphry-Baker, R.; Curchod, B. F. E.; Ashari-Astani, N.; Tavernelli, I.; Rothlisberger, U.; Nazeeruddin, M. K.; Grätzel, M. Dye-Sensitized Solar Cells with 13% Efficiency Achieved through the Molecular Engineering of Porphyrin Sensitizers. *Nat. Chem.* **2014**, 6, 242–247; DOI:10.1038/nchem.1861.
15. Kakiage, K.; Aoyama, Y.; Yano, T.; Oya, K.; Fujisawa, J. I.; Hanaya, M. Highly-Efficient Dye-Sensitized Solar Cells with Collaborative Sensitization by Silyl-Anchor and Carboxy-Anchor Dyes. *Chem. Commun.* **2015**, 51, 15894-15897; DOI:10.1039/c5cc06759f
16. Mauri, L.; Colombo, A.; Dragonetti, C.; Roberto, D.; Fagnani, F. Recent Investigations on Thiocyanate-Free Ruthenium(II) 2,2′-Bipyridyl Complexes for Dye-Sensitized Solar Cells. *Molecules*. 2021, 26, 7638; DOI:10.3390/molecules26247638.
17. Dang Quang, L. N.; Kaliamurthy, A. K.; Hao, N. H. Co-Sensitization of Metal Based N719 and Metal Free D35 Dyes: An Effective Strategy to Improve the Performance of DSSC. *Opt. Mater. (Amst).* **2021**, 111, 110589; DOI:10.1016/j.optmat.2020.110589.
18. Elmorsy, M. R.; Su, R.; Abdel-Latif, E.; Badawy, S. A.; El-Shafei, A.; Fadda, A. A. New Cyanoacetanilides Based Dyes as Effective Co-Sensitizers for DSSCs Sensitized with Ruthenium (II) Complex (HD-2). *J. Mater. Sci. Mater. Electron.* **2020**, 31, 7981–7990; DOI:10.1007/s10854-020-03337-3.
19. Younas, M.; Harrabi, K. Performance Enhancement of Dye-Sensitized Solar Cells via Co-Sensitization of Ruthenium (II) Based N749 Dye and Organic Sensitizer RK1. *Sol. Energy* **2020**, 203, 260-266; DOI:10.1016/j.solener.2020.04.051.
20. Singh A, Singh AK, Dixit R, Vanka K, Krishnamoorthy K, Nithyanandhan J. *ACS Appl. Energy Mater*, 2024, **7 (4)**, 1461-1475
21. Elmorsy, M. R.; Badawy, S. A.; Alzahrani, A. Y. A.; El-Rayyes, A. Molecular Design and Synthesis of Acetohydrazonoyl Cyanide Structures as Efficient Dye-Sensitized Solar Cells with Enhancement of the Performance of the Standard N-719 Dye upon Co-Sensitization. *Opt. Mater. (Amst).* **2023**, 135, 113359; DOI:10.1016/j.optmat.2022.113359.

22. Karaoğlan, G. K.; Hışır, A.; Maden, Y. E.; Karakuş, M. Ö.; Koca, A. Synthesis, Characterization, Electrochemical, Spectroelectrochemical and Dye-Sensitized Solar Cell Properties of Phthalocyanines Containing Carboxylic Acid Anchoring Groups as Photosensitizer. *Dye. Pigment.* **2022**, 204, August 2022, 110390; DOI:10.1016/j.dyepig.2022.110390.
23. Koteshwar, D.; Prasanthkumar, S.; Singh, S. P.; Chowdhury, T. H.; Bedja, I.; Islam, A.; Giribabu, L. Effects of Methoxy Group(s) on D-π-A Porphyrin Based DSSCs: Efficiency Enhanced by Co-Sensitization. *Mater. Chem. Front.* **2022**, 6, 580-592; DOI:10.1039/d1qm01450a.
24. Xu, F.; Testoff, T. T.; Wang, L.; Zhou, X. Cause, Regulation and Utilization of Dye Aggregation in Dye-Sensitized Solar Cells. *Molecules*. 2020, 25, 4478; DOI:10.3390/molecules25194478.
25. Mao, L.; Wu, Y.; Jiang, J.; Guo, X.; Heng, P.; Wang, L.; Zhang, J. Rational Design of Phenothiazine-Based Organic Dyes for Dye-Sensitized Solar Cells: The Influence of π-Spacers and Intermolecular Aggregation on Their Photovoltaic Performances. *J. Phys. Chem. C* **2020**, 124, 9233-9242; DOI:10.1021/acs.jpcc.0c01875.
26. Singh, A. K.; Maibam, A.; Javaregowda, B. H.; Bisht, R.; Kudlu, A.; Krishnamurty, S.; Krishnamoorthy, K.; Nithyanandhan, J. Unsymmetrical Squaraine Dyes for Dye-Sensitized Solar Cells: Position of the Anchoring Group Controls the Orientation and Self-Assembly of Sensitizers on the TiO2 Surface and Modulates Its Flat Band Potential. *J. Phys. Chem. C* **2020**, 124, 18436-18451; DOI:10.1021/acs.jpcc.0c05176.
27. Jadhav, M. M.; Vaghasiya, J. V.; Patil, D.; Soni, S. S.; Sekar, N. Synthesis of Novel Colorants for DSSC to Study Effect of Alkyl Chain Length Alteration of Auxiliary Donor on Light to Current Conversion Efficiency. *J. Photochem. Photobiol. A Chem.* **2019**, 377, 119-129; DOI:10.1016/j.jphotochem.2019.03.043.
28. Pradhan, S.; Kurokawa, Y.; Shaban, S.; Pandey, S. S. Squaric Acid Core Substituted Unsymmetrical Squaraine Dyes for Dye-Sensitized Solar Cells: Effect of Electron Acceptors on Their Photovoltaic Performance. *Colorants* **2023**, 2, 654-673; DOI:10.3390/colorants2040034.
29. Vats, A. K.; Roy, P.; Tang, L.; Hayase, S.; Pandey, S. S. Unravelling the Bottleneck of Phosphonic Acid Anchoring Groups Aiming toward Enhancing the Stability and Efficiency of Mesoscopic Solar Cells. *Front. Chem. Sci. Eng.* **2021**, Published online 2021, 1-19; DOI:10.1007/s11705-021-2117-z.
30. Vats, A. K.; Pradhan, A.; Hayase, S.; Pandey, S. S. Synthesis, Photophysical Characterization and Dye Adsorption Behavior in Unsymmetrical Squaraine Dyes with Varying Anchoring Groups. *J. Photochem. Photobiol. A Chem.* **2020**, 394, 112467; DOI:10.1016/j.jphotochem.2020.112467.
31. Pradhan, A.; Sai Kiran, M.; Kapil, G.; Hayase, S.; Pandey, S. S. Synthesis and Photophysical Characterization of Unsymmetrical Squaraine Dyes for Dye-Sensitized Solar Cells Utilizing Cobalt Electrolytes. *ACS Appl. Energy Mater.* **2018**, 1, 4545–4553; DOI:10.1021/acsaem.8b00653.
32. Butnarasu, C.; Barbero, N.; Viscardi, G.; Visentin, S. Unveiling the Interaction between PDT Active Squaraines with CtDNA: A Spectroscopic Study. *Spectrochim. Acta - Part A Mol. Biomol. Spectrosc.* **2021**, 250, 119224; DOI:10.1016/j.saa.2020.119224.
33. Mavileti, S.K.; Bila, G.; Utka, V.; Bila, E.; Kato, T.; Bilyy, R.; Pandey, S.S. *ACS Appl. Bio Mater*. 2024, **7**, 416–428
34. Yang, D.; Jiao, Y.; Huang, Y.; Zhuang, T.; Yang, L.; Lu, Z.; Pu, X.; Sasabe, H.; Kido, J. Two Different Donor Subunits Substituted Unsymmetrical Squaraines for Solution-Processed Small Molecule Organic Solar Cells. *Org. Electron.* **2016**, 32, 179-186; DOI:10.1016/j.orgel.2016.02.009.
35. Ananda Rao, B.; Kim, H.; Son, Y. A. Synthesis of Near-Infrared Absorbing Pyrylium-Squaraine Dye for Selective Detection of Hg2+. *Sensors Actuators, B Chem.* **2013**, 188, 847-856; DOI:10.1016/j.snb.2013.07.073.

36. Jin, B.; Zhang, X.; Zheng, W.; Liu, X.; Zhou, J.; Zhang, N.; Wang, F.; Shangguan, D. Dicyanomethylene-Functionalized Squaraine as a Highly Selective Probe for Parallel G-Quadruplexes. *Anal. Chem.* **2014**, 86, 7063-7070; DOI:10.1021/ac501619v.
37. Mori, K.; Kurokawa, Y.; Mavileti, S. K.; Pandey, S. S. Design, Synthesis, and Photophysical Characterization of Multifunctional Far-Red Squaraine Dyes for Dye-Sensitized Solar Cells. *Phys. Status Solidi Appl. Mater. Sci.* **2023**, 220, 2300254; DOI:10.1002/pssa.202300254.
38. Pham, W.; Lai, W. F.; Weissleder, R.; Tung, C. H. High Efficiency Synthesis of a Bioconjugatable Near-Infrared Fluorochrome. *Bioconjug. Chem.* **2003**, 14, 1048-1051; DOI:10.1021/bc034070h.
39. Pandey, S. S.; Inoue, T.; Fujikawa, N.; Yamaguchi, Y.; Hayase, S. Substituent Effect in Direct Ring Functionalized Squaraine Dyes on near Infra-Red Sensitization of Nanocrystalline TiO_2 for Molecular Photovoltaics. *J. Photochem. Photobiol. A Chem.* **2010**, 214, 269-275; DOI:10.1016/j.jphotochem.2010.07.010.
40. Periyasamy, K.; Sakthivel, P.; Venkatesh, G.; Vennila, P.; Sheena Mary, Y. Synthesis and Design of Carbazole-Based Organic Sensitizers for DSSCs Applications: Experimental and Theoretical Approaches. *Chem. Pap.* **2024**, 78, 447-461; DOI:10.1007/s11696-023-03101-x.
41. Mishra, A.; Behera, R. K.; Behera, P. K.; Mishra, B. K.; Behera, G. B. Cyanines during the 1990s: A Review. *Chem. Rev.* **2000**, 100, 1973-2011; DOI:10.1021/cr990402t.
42. Yum, J. H.; Moon, S. J.; Humphry-Baker, R.; Walter, P.; Geiger, T.; Nüesch, F.; Grätzel, M.; Nazeeruddin, M. D. K. Effect of Coadsorbent on the Photovoltaic Performance of Squaraine Sensitized Nanocrystalline Solar Cells. *Nanotechnology* **2008**, 19, 424005; DOI:10.1088/0957-4484/19/42/424005.
43. Hwang, B.; Park, M. S.; Kim, K. Ferrocene and Cobaltocene Derivatives for Non-Aqueous Redox Flow Batteries. *ChemSusChem* **2015**, 8, 310-314; DOI:10.1002/cssc.201403021.
44. Ogomi, Y.; Kato, T.; Hayase, S. Dye Sensitized Solar Cells Consisting of Ionic Liquid and Solidification. *J. Photopolym. Sci. Technol.* **2006**, 19, 403-408; DOI:10.2494/photopolymer.19.403.
45. Morimoto, T.; Fujikawa, N.; Ogomi, Y.; Pandey, S. S.; Ma, T.; Hayase, S. Design of Far-Red Sensitizing Squaraine Dyes Aiming towards the Fine Tuning of Dye Molecular Structure. *J. Nanosci. Nanotechnol.* **2016**, 16, 3282-3288(7); DOI:10.1166/jnn.2016.12304.
46. Khazraji, A. C.; Hotchandani, S.; Das, S.; Kamat, P. V. Controlling Dye (Merocyanine-540) Aggregation on Nanostructured TiO_2 Films. An Organized Assembly Approach for Enhancing the Efficiency of Photosensitization. *J. Phys. Chem. B* **1999**, 103, 4693–4700; DOI:10.1021/jp9903110.
47. Bhatt, P.; Pandey, K.; Yadav, P.; Tripathi, B.; Kumar, M. Impedance Spectroscopic Investigation of the Degraded Dye-Sensitized Solar Cell Due to Ageing. *Int. J. Photoenergy* **2016**, 2016, 8523150; DOI:10.1155/2016/8523150.
48. Sarker, S.; Ahammad, A. J. S.; Seo, H. W.; Kim, D. M. Electrochemical Impedance Spectra of Dye-Sensitized Solar Cells: Fundamentals and Spreadsheet Calculation. *International Journal of Photoenergy*. **2014**, 2014, 851705; DOI:10.1155/2014/851705.
49. Hao, F.; Lin, H.; Zhang, J.; Zhuang, D.; Liu, Y.; Li, J. Influence of Iodine Concentration on the Photoelectrochemical Performance of Dye-Sensitized Solar Cells Containing Non-Volatile Electrolyte. *Electrochim. Acta* **2010**, 55, 7225-7229; DOI:10.1016/j.electacta.2010.06.079.
50. Mathew, A.; Anand, V.; Rao, G. M.; Munichandraiah, N. Effect of Iodine Concentration on the Photovoltaic Properties of Dye Sensitized Solar Cells for Various I_2/LiI Ratios. *Electrochim. Acta* **2013**, 87, 92-96; DOI:10.1016/j.electacta.2012.08.104.

 doi:10.20944/preprints202404.1520.v1

51. Datta, J.; Bhattacharya, A.; Kundu, K. K. Relative Standard Electrode Potentials of I_3^-/I^-, I_2/I_3^-, and I_2/I^- Redox Couples and the Related Formation Constants of I_3^- in Some Pure and Mixed Dipolar Aprotic Solvents. *Bull. Chem. Soc. Jpn.* **1988**, 61, 1735-1742; DOI:10.1246/bcsj.61.1735.
52. Nelson, I. V.; Iwamoto, R. T. Voltammetric Evaluation of the Stability of Trichloride, Tribromide, and Triiodide Ions in Nitromethane, Acetone, and Acetonitrile. *J. Electroanal. Chem.* **1964**, 7, 218-221; DOI:10.1016/0022-0728(64)80015-2.